

Sixth-Sense: Self-Supervised Learning of Spatial Awareness of Humans from a Planar Lidar

Simone Arreghini, Nicholas Carlotti, Mirko Nava, Antonio Paolillo, and Alessandro Giusti

Abstract—Localizing humans is a key prerequisite for any service robot operating in proximity to people. In these scenarios, robots rely on a multitude of state-of-the-art detectors usually designed to operate with RGB-D cameras or expensive 3D LiDARs. However, most commercially available service robots are equipped with cameras with a narrow field of view, making them blind when a user is approaching from other directions, or inexpensive 1D LiDARs whose readings are difficult to interpret. To address these limitations, we propose a self-supervised approach to detect humans and estimate their 2D pose from 1D LiDAR data, using detections from an RGB-D camera as a supervision source. Our approach aims to provide service robots with spatial awareness of nearby humans. After training on 70 minutes of data autonomously collected in two environments, our model is capable of detecting humans omnidirectionally from 1D LiDAR data in a novel environment, with 71% precision and 80% recall, while retaining an average absolute error of 13 cm in distance and 44° in orientation.

Index Terms—Self-Supervised Learning, Human Perception, Service Robotics, Human-Robot Interaction.

I. INTRODUCTION

SERVICE robots operating human-populated environments [1]–[3] must be capable to perceive humans, predict their behavior [4] and even intentions [5]. Indeed, humans’ detection and localization are crucial for Human-Robot Interaction (HRI) applications where humans and robots are close, to ensure safe cooperation, improve navigation in crowded spaces, and provide insightful social cues. A typical sensing setup for service robots includes a combination of a wide Field of View (FOV) laser sensor, often seeing 360° around the robot, and a narrow FOV RGB-D camera. Despite 3D LiDAR sensors offering rich information about the surroundings [6], their use in service robots is limited to a small percentage of high-end platforms. Instead, the majority is equipped with simpler 1D planar LiDAR sensors, typically located at wheel height, striking a balance between production costs and richness of information. Examples span from large research robots [7] to those commonly present in many households such as robot vacuum cleaners, or lawnmowers [8].

Deep learning models capable of reliably detecting and localizing humans from RGB-D data have been extensively investigated in literature [9], [10]; however, doing the same with 1D laser sensors remains an open problem due to the sparse nature and complex interpretation of the sensor’s

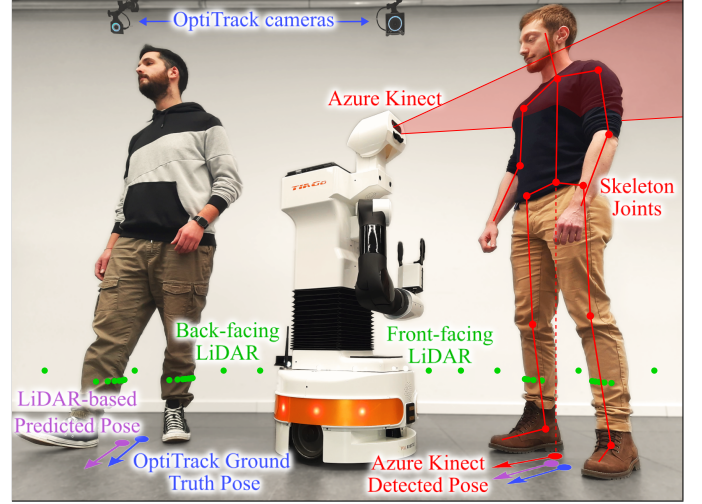


Fig. 1. Our approach uses a human detector from the narrow FOV **Azure Kinect** as a source of labels to train a **1D FCN** that, given planar **LiDAR** scans, predicts the presence and relative 2D pose of humans around the robot. The training approach relies only on hardware onboard the robot and can autonomously collect data in any environment. In this environment (*Lab*), a **Motion Capture** system collects ground truth used for evaluation purposes.

readings. Notably, the typical environment for a service robot may feature structures that result in readings mimicking the profile of human beings, such as the legs of tables, bars in railings, or pets; differentiating humans from the rest requires recognizing subtle geometric and dynamic patterns. Nonetheless, awareness of the presence and direction of nearby humans significantly improves the robot’s behavior in social contexts [11], even when these perceptions are uncertain and possibly inaccurate. Indeed, inspired by animal perception where peripheral vision and hearing direct visual focus towards areas of interest [12], a robot could use uncertain detections from 1D LiDAR data to trigger further sensing by the more reliable RGB-D camera. Unlike previous approaches that rely on 3D LiDAR [13], [14], we handle a less informative sensing modality, leading to inherently lower detection accuracy but with a potential widespread adoption by many robotic platforms.

Our approach relies on a deep learning model that can be trained, or fine-tuned, directly by the robot during its deployment using self-supervision: an off-the-shelf detector receiving data from the onboard RGB-D camera is used to provide detections of humans considered as training labels, as shown in Fig. 1. This is an instance of the general class of approaches using one sensor to supervise the training of a model which interprets data from a different sensor [15], [16]; the same paradigm has been applied to skeleton joint pose esti-

All authors are with the Dalle Molle Institute for Artificial Intelligence (IDSIA), USI-SUPSI, Lugano, Switzerland. Corresponding author: Simone Arreghini, simone.arreghini@supsi.ch

This work was supported by the European Union through the project SER-MAS, by the Swiss State Secretariat for Education, Research and Innovation (SERI) under contract number 22.00247, and by the Swiss National Science Foundation, grant number 213074.

mation from 3D LiDAR, using an image-based human detector providing the 2D skeleton joints pose as supervision [17].

Our model receives as input a moving time window of 1D LiDAR scans and predicts the presence and 2D pose (2D position and relative bearing) of humans around the robot. Specifically, we employ a loss function to minimize the distance between the model’s predicted detections from 1D LiDAR and those coming from the detector, enforced only where the two fields of view overlap. In this context, the self-supervised learning paradigm: allows the model to adapt to the specific deployment environment and sensor characteristics; eliminates the need for large-scale pre-collected datasets; and is robust to cluttered environments that generate scans falsely mimicking human presence. Further, we adopt a 1D FCN [18] and leverage its translation-invariance to extend the detection ability to the wider FOV of the LiDAR sensor, even in directions never covered by the camera.

We describe our **main contribution** in Section II: a practical methodology and open-source implementation for training and running a human detector and pose estimator from 1D LiDAR data using camera detections as self-supervision. As a secondary contribution, datasets collected using this setup, as well as the pre-trained models resulting from our approach, are made publicly available. Section III details the experimental setup comprising our platform, sensing setup, data collection, and network architecture. Section IV presents the quantitative analysis of our approach’s performance against the ground truth, while deployed on a TIAGo robot equipped with an Azure Kinect camera and two 1D LiDAR sensors. Section V concludes the article with final remarks and a discussion on future research directions.

II. METHODOLOGY

We train a 1D FCN model on the task of estimating 2D poses of humans around the robot, giving as input a time window of readings from a planar LiDAR sensor located at the center of the robot base with a uniform angular resolution across the entire FOV. In practice, we use a tensor of 360 elements representing rays equally spaced around the robot with a resulting angular resolution of 1° , and having n channels as the time window history length. We reproject past measurements as if they were captured from the robot’s current position accounting for the robot’s motion as estimated by its

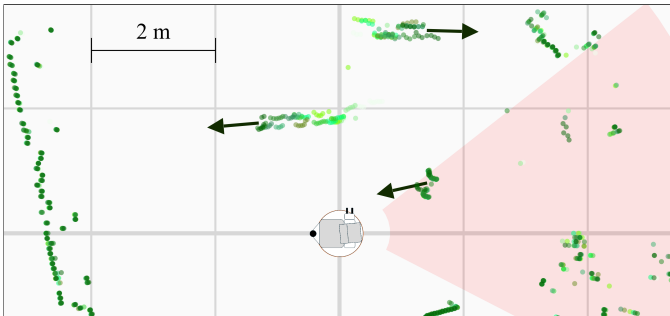


Fig. 2. Walking people and static structures as perceived by the LiDAR: lighter shades of green indicate older scans in the temporal window, whereas black arrows indicate the people’s instantaneous orientation.

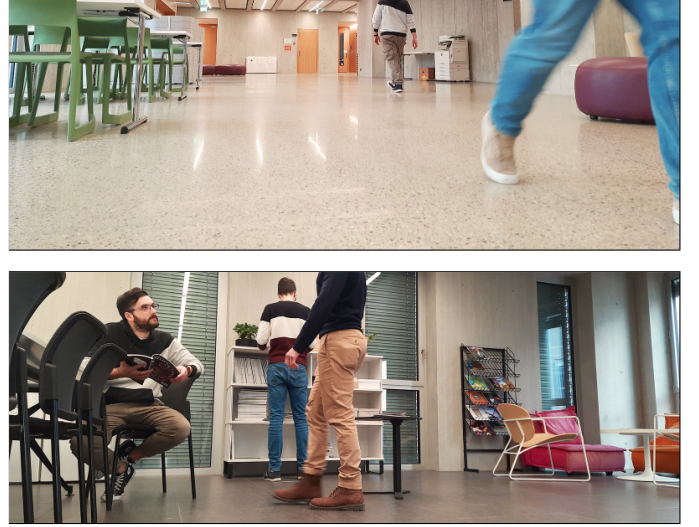


Fig. 3. Training data is autonomously collected by the robot in a *University Corridor*, on the top, and a *Break Area*, on the bottom.

odometry. As a result, static obstacles yield overlapping points across the channels, while moving obstacles leave trail-like point patterns, as shown in Fig. 2. The model is tasked to predict the presence of humans in the environment, and their distance and bearing relative to the robot. For each ray, our model predicts: the scalar $\hat{p} \in [0, 1]$ representing the likelihood of human presence; the relative distance $\hat{d} \in [d_{\min}, d_{\max}]$, where d_{\min} and d_{\max} are the working range of the sensor; and the sine and cosine of the relative bearing $\hat{o} \in [-\pi, \pi]$ expressed as the difference between the person’s orientation and the direction parallel to the ray, with zero indicating a person directly facing the robot. During inference, a discrete set of detections is obtained by thresholding and applying Non-maxima Suppression (NMS) to the model’s predicted presence. We aim to extend the detection ability of the model from the narrow area covered by the camera’s FOV to the wider LiDAR’s FOV, including areas where the supervision is scarce or absent, such as behind the robot. To this end, we rely on the translational invariance of convolutions, in which patterns are detected regardless of their position within the input.

The self-supervision signal is derived from the front-facing onboard camera providing the 3D pose of people’s joints in the camera’s FOV. Among the joints, we specifically select the one located at the pelvis as it’s closely tied to the legs’ motion, and project its pose onto the horizontal plane to get 2D poses. Labels for human presence p , distance d , and relative bearing o are obtained from such poses for each ray of the LiDAR scan intersecting a person. The presence p is set to 1 when a person is detected along the ray, or 0 otherwise; accordingly, the relative distance and bearing labels of people are assigned to rays in which they are detected, or left undefined otherwise. Our model is trained to regress the three components using a masked loss, considering only errors generated from the rays corresponding to the area covered by the camera’s FOV. Additionally, distance and orientation losses are computed only for rays in which the supervision labels indicate the presence of humans.

III. EXPERIMENTAL SETUP

A. Hardware

We use a customized version of the PAL Robotics TIAGo robot composed of a differential drive base, a torso with a prismatic joint, a 7 degrees-of-freedom manipulator, and a head that can pan in the range $\pm 75^\circ$ and tilt from -60° to 45° w.r.t. the horizontal plane. Our TIAGo is equipped with additional sensors to better suit HRI applications: a Microsoft Azure Kinect RGB-D camera located in the head reliably tracks humans up to 6 m [10], has a narrow horizontal FOV of 65° , and frame rate of 15 Hz; a secondary LiDAR sensor mounted on the back of the robot's base, in addition to the built-in one located on the front, as shown in Fig. 1. The front-facing LiDAR is at an height of 95 mm, has a FOV of 190° , and scan rate of 15 Hz; the back-facing one is at an height of 329 mm, FOV of 255° , and scan rate of 10 Hz; both sensors' operating range goes from 0.05 m to 10 m. To obtain a single, omnidirectional, and radially symmetric sensor, we fuse the two physical LiDARs into a *virtual* one: the two sensors' readings are time-synchronized at a rate of 10 Hz, projected onto the 2D plane, expressed in the frame of the robot base, and aggregated into 1° -wide bins; each bin is assigned the value of the closest point among its members; when there are no members, a default value of 10 m is used.

B. Dataset

We collected data across 9 days in three environments: *University Corridor* (shown in Fig. 3, top), a public transit area between classrooms with study desks on the side and passers-by (36k samples); *Break Area* (Fig. 3, bottom), a large room with tables and chairs where expert individuals interact with the robot (12k samples); and *Lab* (Fig. 1), a laboratory setting with expert individuals interacting with the robot (7k samples). During data collection, the robot's base motion and the head panning are randomized to increase the data variability and area covered by the camera. The robot base is manually controlled in the *University Corridor* for security reasons whereas, in the other environments, it moves autonomously following random trajectories while avoiding collisions. In all environments, we record body joints from the Azure Kinect and scans from the two LiDARs. Additionally, the *Lab* environment provides ground truth poses for people and the robot at 100 Hz from an OptiTrack motion capture system featuring 18 cameras. The data is split into a training set composed of all samples from *University Corridor* and half of those from *Break Area*, totaling 42k samples; the remaining 6k samples from *Break Area* are used as validation set, and the 7k samples from *Lab* are used as the test set.

C. Model architecture

Our model, depicted in Fig. 4, is composed of 7 1D convolutional layers, each with 32 output channels and layer normalization. It features dilated circular convolutions with increasing kernel dimension from 3 to 7, resulting in a receptive field of 43° . Specifically, dilation is used to have a low model complexity while achieving a receptive field large enough to

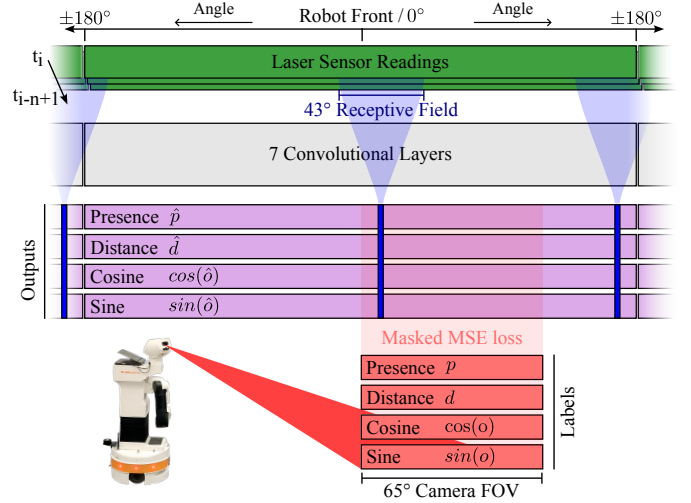


Fig. 4. Our model uses a temporal window of n LiDAR scans to predict the presence p of nearby people, their distance d , and relative bearing o (represented by sine and cosine). Dilated circular convolutions handle omnidirectional scans and yield a 43° receptive field. A masked MSE loss is only enforced on predictions that overlap with the camera FOV (red shaded area).

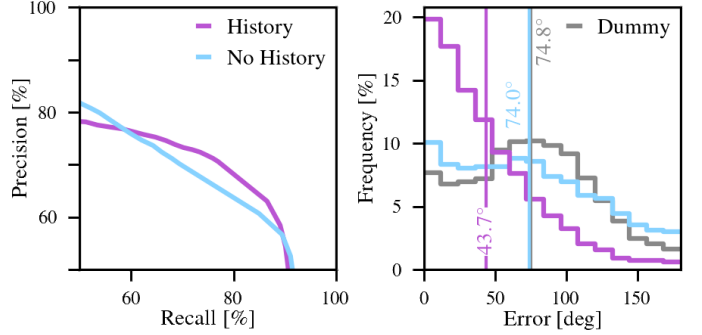


Fig. 5. Left: Precision-Recall curve for detection. Right: relative bearing error distribution. Results computed against mocap ground truth in the *Lab* test set.

effectively capture human motion. During training, the model minimizes a squared error between predictions and label values of each output. We train our model for 500 epochs at a constant learning rate of $3e^{-4}$ using the Adam optimizer [19] and select the model weights resulting in the lowest validation loss. We apply additive Gaussian noise and mirroring to the input as data augmentations during model training.

IV. RESULTS

We compare our model using the last $n = 30$ scans collected at 10 Hz over three seconds, called *History*, with an ablated baseline named *No History* that uses only the current sensor reading as input ($n = 0$). All models are tested using the ground truth poses collected in the *Lab* environment, as shown in Fig. 1. On the left of Fig. 5, we report the Precision-Recall curve illustrating the human detection performance of our models. This curve is generated by progressively increasing the detection threshold applied to the presence output \hat{p} . Human's predicted positions are obtained by projecting a point in the direction of the corresponding ray at the estimated distance \hat{d} . A prediction is considered a match (true positive) when it has an Euclidean distance smaller than 50 cm w.r.t. the ground

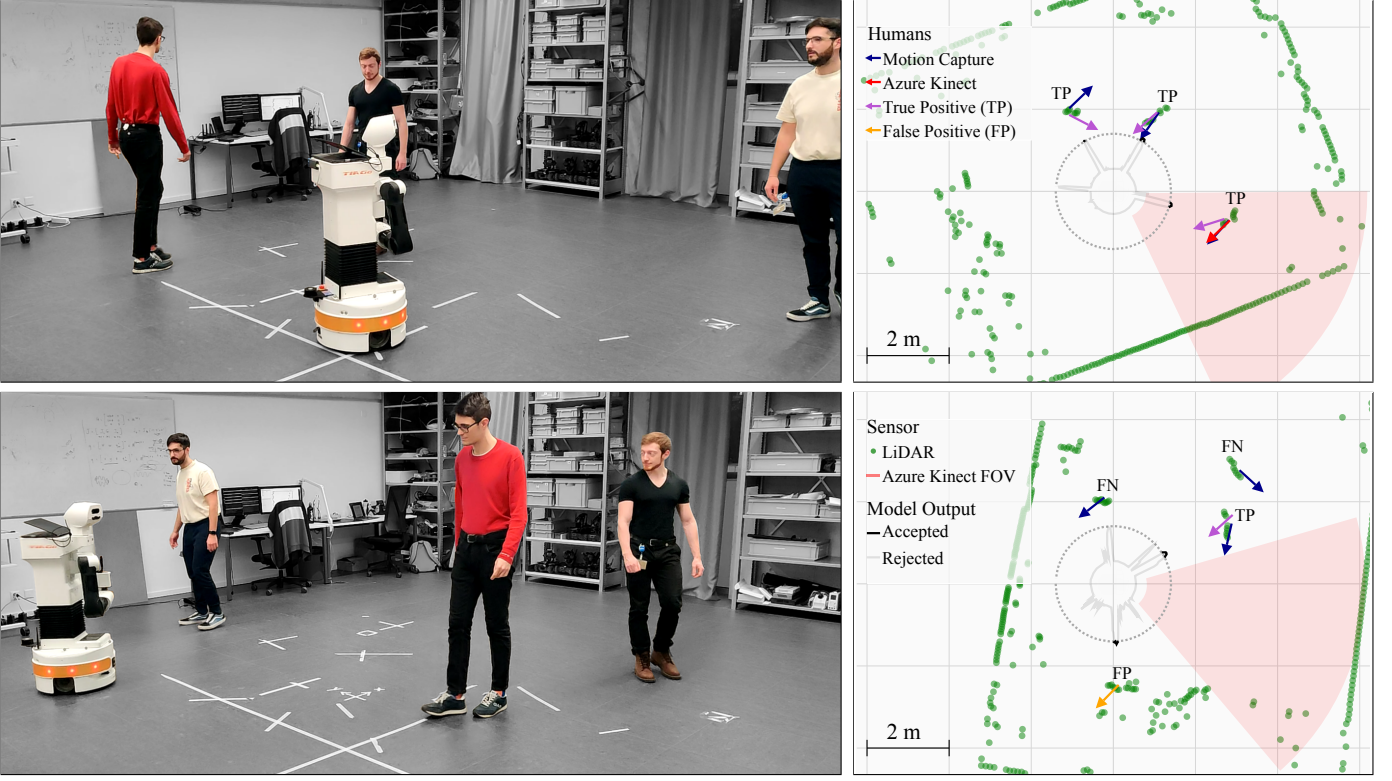


Fig. 6. Results on the test set: third-person view of two frames (left) and corresponding top view (right) depicting the LiDAR scan; camera FOV and detected pose arrows; Motion Capture ground truth pose arrows. The predicted presence \hat{p} is shown as a gray line when below the detection threshold of 90% (dashed circle centered on the robot), or black otherwise. Predictions are represented by arrows colored differently for true positives (TP), and false positives (FP).

truth; the orientation component does not influence the matching procedure. The plot shows that, for recall values above 60%, the *History* model (in purple) consistently outperforms *No History* (in light blue). On the right of Fig. 5, we compare the orientation error distributions. We include a *Dummy* model that always returns the average ground truth orientation and distance in the test set. Errors are computed only for matched predictions (true positives), following the same approach used for the Precision-Recall curve; for the *Dummy* model, instead, we consider the whole test set, i.e., assuming an ideal detection. Results show that temporal information is required for relative bearing estimation: *History* yields a mean absolute orientation error of 44° compared to *No History* with 74° and *Dummy* with 75° ; this result confirms the findings in the literature on the human motion model [20], [21].

The qualitative performance of our approach on detection and 2D pose estimation are shown in Fig. 6, with the TIAGo robot deployed in the *Lab* environment. Failed detections derive from the choice of threshold yielding false negatives for high predictions that fall below the threshold. Table I summarizes the models' performance with the following metrics: for human detection, we report the precision on the true positive predictions corresponding to the threshold yielding a recall of 80%, represented as P_{80} , where the *History* model outperforms *No History* by scoring $P_{80} = 70.6\%$ against $P_{80} = 60.7\%$. On the true positive predictions, we additionally measure the mean orientation E_o and distance E_d absolute errors.

TABLE I
MODELS' PERFORMANCE ON HUMAN DETECTION P_{80} , MEAN RELATIVE BEARING ERROR E_o , AND MEAN DISTANCE ERROR E_d ON THE TEST SET.

Model	P_{80} [%] \uparrow	E_o [deg] \downarrow	E_d [cm] \downarrow	Barplot for P_{80} [%] \rightarrow
<i>Dummy</i>	—	75	64	
<i>No History</i>	60.7	74	10	
<i>History</i>	70.6	42	13	

V. CONCLUSION

We presented a novel approach for human detection and pose estimation in service robots using 1D LiDAR sensors. It leverages a state-of-the-art detector from an RGB-D camera as the source of self-supervision, requiring no pre-collected datasets. This approach can adapt to different sensing setups, assuming only to have a precise albeit narrow source of supervision for interpreting readings from a much wider FOV, possibly omnidirectional sensor. The code required to collect data, train models, and run them in real time is made publicly available for the benefit of the community; we also provide pre-trained model weights and datasets. Future work will focus on the use of pretext tasks to leverage unlabeled data at training time, and extend the model predictions with more complex social cues, such as the intention to interact, which could be highly beneficial in human-robot interaction scenarios.

REFERENCES

- [1] F. B. V. Benitti, "Exploring the educational potential of robotics in schools: A systematic review," *Comp. & Education*, vol. 58, no. 3, pp. 978–988, 2012.
- [2] C. S. González-González, V. Violant-Holz, and R. M. Gil-Iranzo, "Social robots in hospitals: a systematic review," *Appl. Sci.*, vol. 11, no. 13, p. 5976, 2021.
- [3] M. M. O. Youngjoon Choi, Miju Choi and S. S. Kim, "Service robots in hotels: understanding the service quality perceptions of human-robot interaction," *J. of Hospitality Marketing & Management*, vol. 29, no. 6, pp. 613–635, 2020.
- [4] A. Zarak, M. Giuliani, M. B. Dehkordi, D. Mazzei, A. D'ursi, and D. De Rossi, "An RGB-D based social behavior interpretation system for a humanoid social robot," in *RSI/ISM Int. Conf. on Robot. and Mechatronics*, 2014, pp. 185–190.
- [5] S. Arreghini, G. Abbate, A. Giusti, and A. Paolillo, "Predicting the intention to interact with a service robot: the role of gaze cues," in *IEEE Int. Conf. Robot. and Autom.*, 2024, pp. –.
- [6] R. Martin-Martin, M. Patel, H. Rezatofighi, A. Sheno, J. Gwak, E. Frankel, A. Sadeghian, and S. Savarese, "Jrdb: A dataset and benchmark of egocentric robot visual perception of humans in built environments," *IEEE Trans. on Pattern Anal. and Machine Intell.*, vol. 45, no. 6, pp. 6748–6765, 2021.
- [7] J. Pages, L. Marchionni, and F. Ferro, "TIAGo: the modular robot that adapts to different research needs," in *International workshop on robot modularity, IROS*, vol. 290, 2016.
- [8] H. Mahdi, S. A. Akgun, S. Saleh, and K. Dautenhahn, "A survey on the design and evolution of social robots—past, present and future," *Elsevier Robotics and Autonomous Systems*, vol. 156, p. 104193, 2022.
- [9] M. Paul, S. M. Haque, and S. Chakraborty, "Human detection in surveillance videos and its applications-a review," *Springer Journal on Advances in Signal Processing*, vol. 2013, no. 1, pp. 1–16, 2013.
- [10] M. Tölgyessy, M. Dekan, and L. Chovanec, "Skeleton tracking accuracy and precision evaluation of kinect v1, kinect v2, and the azure kinect," *MDPI Applied Sciences*, vol. 11, no. 12, p. 5756, 2021.
- [11] N. K. Dhiman, D. Deodhare, and D. Khemani, "Where am i? creating spatial awareness in unmanned ground robots using slam: A survey," *Springer Sadhana*, vol. 40, pp. 1385–1433, 2015.
- [12] M. D. Vernon, "The peripheral perception of movement," *Cambridge University Press British Journal of Psychology*, vol. 23, no. 3, p. 209, 1933.
- [13] Z. Yan, T. Duckett, and N. Bellotto, "Online learning for 3d lidar-based human detection: experimental analysis of point cloud clustering and classification methods," *Springer Autonomous Robots*, vol. 44, no. 2, pp. 147–164, 2020.
- [14] J. N. Hayton, T. Barros, C. Prenebida, M. J. Coombes, and U. J. Nunes, "Cnn-based human detection using a 3d lidar onboard a uav," in *IEEE Int. Conf. Auton. Robot. Sys. and Comp.*, 2020, pp. 312–318.
- [15] M. Nava, J. Guzzi, R. O. Chavez-Garcia, L. M. Gambardella, and A. Giusti, "Learning long-range perception using self-supervision from short-range sensors and odometry," *IEEE Robot. and Autom. Lett.*, vol. 4, no. 2, pp. 1279–1286, 2019.
- [16] M. Nava, A. Paolillo, J. Guzzi, L. M. Gambardella, and A. Giusti, "Uncertainty-aware self-supervised learning of spatial perception tasks," *IEEE Robot. and Autom. Lett.*, vol. 6, no. 4, pp. 6693–6700, 2021.
- [17] P. Cong, Y. Xu, Y. Ren, J. Zhang, L. Xu, J. Wang, J. Yu, and Y. Ma, "Weakly supervised 3d multi-person pose estimation for large-scale scenes based on monocular camera and single lidar," in *AAAI Conference on Artificial Intelligence*, vol. 37, no. 1, 2023, pp. 461–469.
- [18] J. Long, E. Shelhamer, and T. Darrell, "Fully convolutional networks for semantic segmentation," in *IEEE/CVF Conf. on Comp. Vision and Pattern Recogn.*, 2015, pp. 3431–3440.
- [19] D. P. Kingma and J. Ba, "Adam: a method for stochastic optimization," in *Int. Conf. on Learn. Represent.*, 2015.
- [20] W. Liu, Y. Zhang, S. Tang, J. Tang, R. Hong, and J. Li, "Accurate estimation of human body orientation from rgb-d sensors," *IEEE Trans. on Cybernetics*, vol. 43, no. 5, pp. 1442–1452, 2013.
- [21] Z. Luo, S. A. Golestaneh, and K. M. Kitani, "3d human motion estimation via motion compression and refinement," in *Asian Conference on Computer Vision*, 2020.

TABLE II
DESCRIPTION OF SUPPLEMENTARY MATERIALS

Supplementary material	Description
Zenodo Dataset Link	Link to the Zenodo page for the publicly available dataset. The excessive size of our dataset prevents direct upload. Further dataset explanation is available at the linked page. URL: https://zenodo.org/records/14936069
IEEE DataPort Link	Link to the IEEE DataPort page for the publicly available dataset. URL: https://iee-dataport.org/documents/sixth-sense-indoor-human-spatial-awareness-dataset